Echo chambers and opinion dynamics explain the occurrence of vaccination hesitancy *

Johannes Müller, Aurélien Tellier, Michael Kurschilgen

September 18, 2022

A Supplementary Material

A.1 Analytical results: Deterministic limit

We present here the results of the deterministic limit.

Theorem A.1 *Let $x_k(t) = X^{(k)}(t)/N$, $n_i = N_i/N$. Then, the deterministic limit of the model is given by the ODE*

$$\dot{x}_k = \mu\left(- \frac{\vartheta_2\, x_k\, ((1-\hat{x}_k)+n_2)}{(\hat{x}_k+n_1)+\vartheta_2((1-\hat{x}_k)+n_2)} + \frac{\vartheta_1\,(1-x_k)\,(\hat{x}_k+n_1)}{\vartheta_1(\hat{x}_k+n_1)+((1-\hat{x}_k)+n_2)}\right) \tag{1}$$

$$\hat{x}_k = (1-\tau)x_k + \frac{\tau}{d_k}\sum_{k'\sim k} x_{k'}. \tag{2}$$

Proof: Let $X_t = (X_t^{(k)})_{k\in\Gamma}$, and $x(t) = (X_t^{(k)}/N)_{k\in\Gamma}$. The rates to increase/decrease the state $X_t^{(k)}$ can be written as $f_{+,k}(X_t/N)$ resp. $f_{-,k}(X_t/N)$, where

$$f_{+,k}(x) = \mu(1-x_k)\,\frac{\vartheta_1(\hat{x}_k+n_1)}{\vartheta_1(\hat{x}_k+n_1)+(1-\hat{x}_k+n_2)}, \qquad f_{-,k}(x) = \mu x_k\,\frac{\vartheta_2(1-\hat{x}_k+n_2)}{(\hat{x}_k+n_1)+\vartheta_2(1-\hat{x}_k+n_2)}.$$

$\hat{x}_k$ is defined in the statement of the theorem. Therewith, the Kramers-Moyal expansion yields the limiting Fokker-Planck equation for the probability density $\psi(x,t)$

$$\partial_t\psi(x,t) = -\sum_{k\in\Gamma}\partial_{x^{(k)}}\left(\left(f_{+,k}(x)-f_{-,k}(x)\right)\psi(x,t)\right) + \frac{1}{2N}\sum_{k\in\Gamma}\partial^2_{x^{(k)}}\left(\left(f_{+,k}(x)+f_{-,k}(x)\right)u(x,t)\right)$$

The deterministic ODE is determined by the drift term, such that $\dot{x}_k = f_{+,k}(x) - f_{-,k}(x)$. This yields the desired result. □

* J. Müller is affiliated to the Technical University of Munich and the Helmholtzzentrum Munich (johannes.mueller@mytum.de), A. Tellier is affiliated to the Technical University of Munich (aurelien.tellier@tum.de), and M. Kurschilgen is affiliated to the Technical University of Munich, the Max Planck Institute for Research on Collective Goods, and the Stanford Graduate School of Business (m.kurschilgen@tum.de)

A.2 Analytical results: Proof of Proposition 3.1 (main text)

Proof: We start with the Fokker-Planck equation obtained by the Kramers-Moyal expansion, where we use the scaling $n_i = N_i/N$, and ϑ_i constant in N. Only afterwards, we proceed to the desired scaling.

As seen above, the rates to increase/decrease the state can be written as $f_+(X_t/N)$ resp. $f_-(X_t/N)$, where

$$f_+(x) = \mu(1-x)\,\frac{\vartheta_1(x+n_1)}{\vartheta_1(x+n_1)+(1-x+n_2)}, \qquad f_-(x) = \mu x\,\frac{\vartheta_2(1-x+n_2)}{(x+n_1)+\vartheta_2(1-x+n_2)}.$$

As we are in a one-patch-model (no spatial structure), we do not have an index k, and also no variable $\hat{x}$ that is responsible for the communication between patches. Therewith, the limiting Fokker-Planck equation reads

$$\partial_t u(x,t) = -\partial_x((f_+(x)-f_-(x))\,u(x,t)) + \frac{1}{2N}\partial_x^2((f_+(x)+f_-(x))\,u(x,t))$$

Now we rewrite drift and noise term with the new scaling $n_i = N_i/N$, $\vartheta_i = 1-\theta_i/N$, where we neglect terms of order $\mathcal{O}(N^{-2})$. We find (using the computer-algebra tool maxima [5]) that ($h := 1/N$)

$$\begin{aligned} & f_+(x) - f_-(x) \\ = \;& \mu(1-x)\,\frac{(1-h\,\theta_1)(x+h\,N_1)}{(1-h\,\theta_1)(x+h\,N_1)+(1-x+h\,N_2)} - \mu x\,\frac{(1-h\,\theta_2)(1-x+h\,N_2)}{(x+h\,N_1)+(1-h\,\theta_2)(1-x+h\,N_2)} \\ = \;& \mu\Big([(\theta_1+\theta_2)x-\theta_1]\,x\,(1-x) - (N_1+N_2)\,x + N_1\Big)\,h + \mathcal{O}(h^2), \end{aligned}$$

while $h(f_+(x)+f_-(x)) = h\,2\,\mu x(1-x) + \mathcal{O}(h^2)$. If we rescale time, $T = \mu\,h\,t$, the Fokker-Planck equation becomes

$$\partial_T u(x,T) = -\,\partial_x\Big\{\;\Big([(\theta_1+\theta_2)x-\theta_1]\,x\,(1-x) - (N_1+N_2)\,x + N_1\Big)\;u(x,T)\;\Big\} + \partial_x^2\Big\{x\,(1-x)\,u(x,T)\Big\}.$$

For the invariant (and stationary) distribution $\varphi(x)$ the flux of that rescaled Fokker-Planck equation is zero, that is,

$$-\Big([(\theta_1+\theta_2)x-\theta_1]\,x\,(1-x) - (N_1+N_2)\,x + N_1\Big)\varphi(x) + \frac{d}{dx}\Big(x(1-x)\,\varphi(x)\Big) = 0.$$

With $v(x) = x(1-x)u(x)$, we have

$$v'(x) = \Big([(\theta_1+\theta_2)x-\theta_1] + \frac{N_1}{x} - \frac{N_2}{1-x}\,x\Big)v(x)$$

and hence

$$v(x) = C\,e^{\frac{1}{2}(\theta_1+\theta_2)x^2-\theta_1 x}\;x^{N_1}\,(1-x)^{N_2}$$

resp.

$$\varphi(x) = C\,e^{\frac{1}{2}(\theta_1+\theta_2)x^2-\theta_1 x}\;x^{N_1-1}\,(1-x)^{N_2-1}$$

□

A.3 Analytical results: Proof of Theorem 3.2 (main text)

Proof: We again start off with the Fokker-Planck equation, obtained by the Kramers-Moyal expansion, where we use the scaling $n_i = N_i/N$, and ϑ_i constant in N. Only afterwards, we proceed to the desired scaling. As seen above, the rates to increase/decrease the state in site k can be written as $f_+^{(k)}(X_t^{(\cdot)}/N)$ resp. $f_-^{(k)}(X_t^{(\cdot)}/N)$, where

$$\begin{aligned} f_+^{(k)}(x^{(\cdot)}) &= \frac{[\mu(1-x^{(k)})]\ [\vartheta_1((1-\tau)\,x^{(k)}+\tau\check{x}^{(k)}+n_1)]}{\vartheta_1((1-\tau)\,x^{(k)}+\tau\check{x}^{(k)}+n_1)+(1-(1-\tau)\,x^{(k)}-\tau\check{x}^{(k)}+n_2)}, \\ f_-^{(k)}(x^{(\cdot)}) &= \frac{[\mu x^{(k)}]\ [\vartheta_2(1-(1-\tau)\,x^{(k)}-\tau\check{x}^{(k)}+n_2)]}{((1-\tau)\,x^{(k)}+\tau\check{x}^{(k)}+n_1)+\vartheta_2(1-(1-\tau)\,x^{(k)}-\tau\check{x}^{(k)}+n_2)}. \end{aligned}$$

Here, $\hat{x}^{(k)}$ is the average of $x^{(\cdot)}$ in the neighborhood of j, given by the graph Γ.

Therewith, the flux $j^{(k)}(x^{(\cdot)})$ for the limiting Fokker-Planck equation is defined by

$$\begin{aligned} j^{(k)}(x^{(\cdot)}) &= -\Big(f_+^{(k)}(x^{(\cdot)})-f_-^{(k)}(x^{(\cdot)})\Big)u(x^{(\cdot)}) \\ &\quad +\frac{1}{2N}\,\partial_{x^{(k)}}\Big\{\Big(f_+^{(k,\ell)}(x^{(\cdot)})+f_-^{(k,\ell)}(x^{(\cdot)})\Big)u(x^{(\cdot)})\Big\} \end{aligned}$$

and the Fokker-Planck equation itself reads

$$\partial_t u(x^{(\cdot)}) = \sum_{k\in\Gamma}\partial_{x^{(k)}} j^{(k)}(x^{(\cdot)}).$$

Now we rewrite drift and noise term with the new scaling $n_i = N_i/N$, $\vartheta_i = 1-\theta_i/N$, $\tau = \gamma/N$, where we neglect terms of order $\mathcal{O}(N^{-2})$. We obtain (again using the computer-algebra program maxima [5]) that ($h := 1/N$)

$$\begin{aligned} & f_+^{(k)}(x^{(\cdot)})-f_-^{(k)}(x^{(\cdot)}) \\ = \ & \frac{\mu\,(1-x^{(k)})\ [\vartheta_1((1-\tau)\,x^{(k)}+\tau\check{x}^{(k)}+n_1)]}{\vartheta_1((1-\tau)\,x^{(k)}+\tau\check{x}^{(k)}+n_1)+(1-(1-\tau)\,x^{(k)}-\tau\check{x}^{(k)}+n_2)} \\ & -\frac{\mu\,x^{(k)}\ [\vartheta_2(1-(1-\tau)\,x^{(k)}-\tau\check{x}^{(k)}+n_2)]}{((1-\tau)\,x^{(k)}+\tau\check{x}^{(k)}+n_1)+\vartheta_2(1-(1-\tau)\,x^{(k)}-\tau\check{x}^{(k)}+n_2)} \\ = \ & \mu\Big((\check{x}^{(k)}-x^{(k)})\,\gamma\ x^{(k)}\,(1-x^{(k)}) \\ & \qquad +x^{(k)}\,(1-x^{(k)})\,(\theta_2\,x^{(k)}-\theta_1\,(1-x^{(k)}))-(N_2+N_1)x^{(k)}+N_1\Big)\,h+\mathcal{O}(h^2), \end{aligned}$$

while $f_+^{(k)}(x^{(\cdot)})+f_-^{(k)}(x^{(\cdot)}) = 2\,\mu\,x^{(k)}\,(1-x^{(k)})+\mathcal{O}(h)$. Hence, in lowest order, $j^{(k)}(x^{(\cdot)}) = 0$ reads

$$\begin{aligned} & \partial_{x^{(k)}}\Big\{\Big(x^{(k)}(1-x^{(k)})\Big)u(x^{(\cdot)})\Big\} \\ = \ & \Big(x^{(k)}\,(1-x^{(k)})\,(\gamma(\check{x}^{(k)}-x^{(k)})+\theta_2\,x^{(k)}-\theta_1\,(1-x^{(k)}))-(N_2+N_1)x^{(k)}+N_1\Big)u(x^{(\cdot)}). \end{aligned}$$

For $\gamma = 0$, this equation collapses to the case without interaction across patches. This observation motivates us to introduce $v(x^{(\cdot)})$ by

$$u(x^{(\cdot)}) = v(x^{(\cdot)}) \prod_{k' \in \Gamma} \varphi(x^{(k')}).$$

Therewith, we obtain

$$\partial_{x^{(k)}} v(x^{(\cdot)}) \quad = \quad \gamma \, (\check{x}^{(k)} - x^{(k)}) \; v(x^{(\cdot)})$$

with the solution

$$v(x^{(\cdot)}) = C \exp\left\{ \gamma \sum_{k \in \Gamma} \left(\frac{1}{2\, d_k} \sum_{k' \sim k} x^{(k)} x^{(k')} - \frac{1}{2} \, (x^{(k)})^2 \right) \right\}.$$

The factor $1/(2\, d_k)$ is due to symmetry reasons: Each pair of nodes (k_1, k_2) with $k_1 \sim k_2$ appears twice in the sum. We rewrite the sum as follows

$$\begin{aligned}
& \sum_{k \in \Gamma} \left(\frac{1}{2\, d_k} \sum_{k' \sim k} x^{(k)} x^{(k')} - \frac{1}{2} \, (x^{(k)})^2 \right) = \sum_{k \in \Gamma} \frac{1}{2\, d_k} \left(\sum_{k' \sim k} x^{(k)} x^{(k')} - d_k \, (x^{(k)})^2 \right) \\
= \; & - \sum_{k \in \Gamma} \frac{1}{2\, d_k} \left(\sum_{k' \sim k} \left(- x^{(k)} x^{(k')} + (x^{(k)})^2 \right) \right) = - \sum_{k \in \Gamma} \frac{1}{2\, d_k} \, \frac{1}{2} \left(\sum_{k' \sim k} \left((x^{(k')})^2 - 2 x^{(k)} x^{(k')} + (x^{(k)})^2 \right) \right) \\
= \; & - \sum_{k \in \Gamma} \frac{1}{4\, d_k} \left(\sum_{k' \sim k} \left(x^{(k)} - x^{(k')} \right)^2 \right).
\end{aligned}$$

□

A.4 Bifurcation analysis

We consider the deterministic scaling (SI, section A.1), but only ocnsider one single patch. If x is the fraction of opinion 1 supporters, the ODE reads (use $\tau = 0$)

$$\dot{x} \quad = \quad -\mu x \, \frac{\vartheta_2 (1 - x + n_2)}{(x + n_1) + \vartheta_2 (1 - x + n_2)} + \mu (1 - x) \, \frac{\vartheta_1 (x + n_1)}{\vartheta_1 (x + n_1) + (1 - x + n_2)}. \tag{3}$$

Proposition A.2 *For $n_1 = n_2 = n$ and $\vartheta_1 = \vartheta_2$, $x = 1/2$ always is a stationary point; this stationary point undergoes a pitchfork bifurcation at $\vartheta_1 = \vartheta_2 = \vartheta_p$, where*

$$\vartheta_p \quad = \quad \frac{1 - 2n}{1 + 2n}. \tag{4}$$

Proof: The rates to increase/decrease the state can be written as $f_+(X_t/N)$ resp. $f_-(X_t/N)$, where (recall that $n_{a/b} = N^{a/b}/N$)

$$f_+(x) = \mu (1 - x) \, \frac{\vartheta_1 (x + n_1)}{\vartheta_1 (x + n_1) + (1 - x + n_2)}, \qquad f_-(x) = \mu x \, \frac{\vartheta_2 (1 - x + n_2)}{(x + n_1) + \vartheta_2 (1 - x + n_2)}.$$

Therewith, the Fokker-Planck equation for the large population size (Kramers-Moyal expansion) reads

$$\partial_t u(x,t) = -\partial_x ((f_+(x) - f_-(x)) \, u(x,t)) + \frac{1}{2N} \partial_x^2 ((f_+(x) + f_-(x)) \, u(x,t))$$

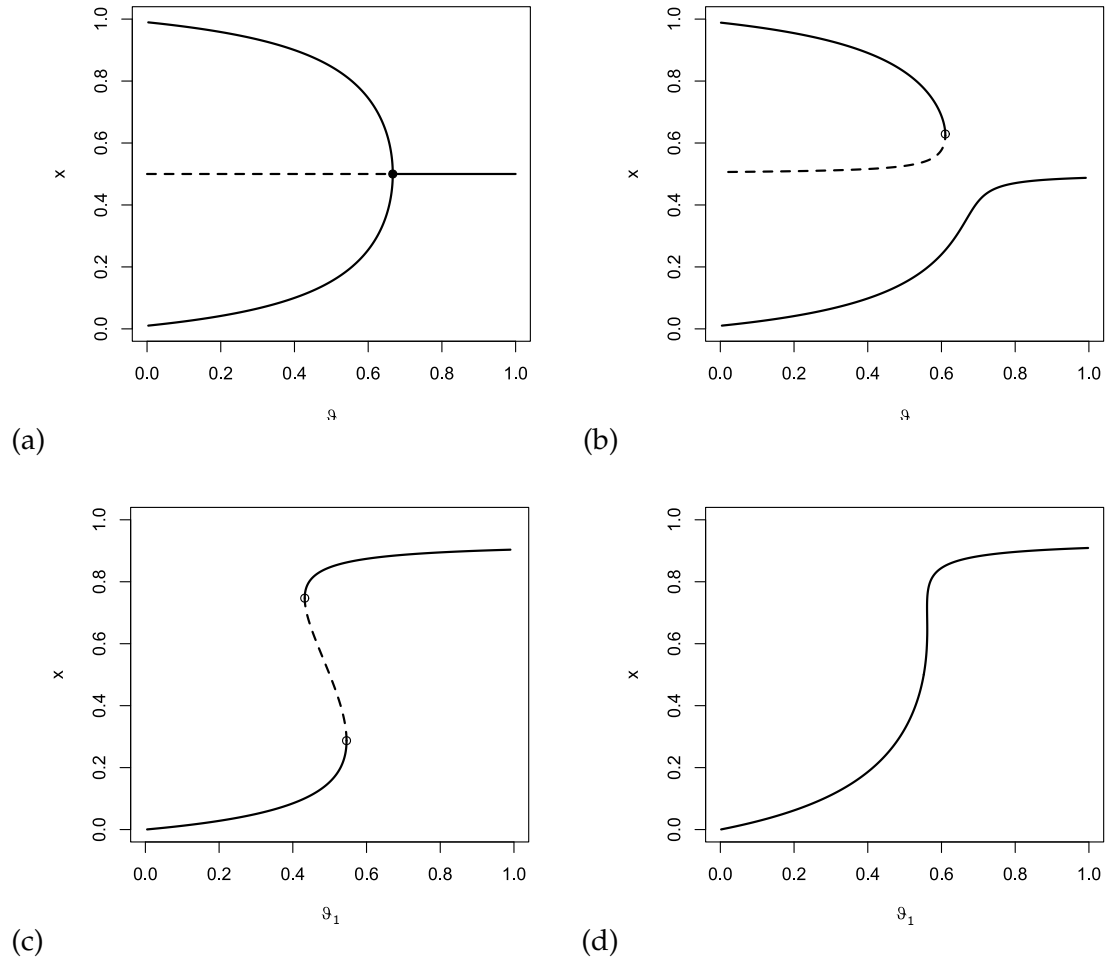

Figure 1: Stationary points of the reinforcement model over $\vartheta = \vartheta_1 = \vartheta_2$. The pitchfork bifurcation in (a) is indicated by a bullet, the saddle-node bifurcations in (b) and (c) are indicated by open circles. Stable branches of stationary points are represented by solid lines, unstable branches by dotted lines. (a) $n_1 = n_2 = 0.1$, $\vartheta_1 = \vartheta_2 = \vartheta$, (b) $n_1 = 0.1$, $n_2 = 0.105$, $\vartheta_1 = \vartheta_2 = \vartheta$, (c) $n_1 = n_2 = 0.1$, reinforcement for group A $\vartheta_2 = 0.5$, ϑ_1 on the x-axis, (d) $n_1 = 0.2$, $n_2 = 0.02$, reinforcement for group A $\vartheta_2 = 1.0$, ϑ_1 on the x-axis.

and the ODE due to the drift term in case of $N \to \infty$ reads

$$\frac{d}{dt}x = f_+(x) - f_-(x).$$

Due to symmetry reasons, if $n_1 = n_2$ and $\vartheta_1 = \vartheta_2$, we find $f_+(1-x) = f_-(x)$ and $f_+(x) = f_-(1-x)$, which implies

$$f_+(1-x) - f_-(1-x) = f_-(x) - f_- + (x) = -(f_+(x) - f_-(x)).$$

Hence, each even number of derivatives of $f_+(x) - f_-(x)$ at $x = 1/2$ yields zero,

$$\frac{d^{2i}}{dx^{2i}}\Big(f_+(1-x) - f_-(1-x)\Big) = -\frac{d^{2i}}{dx^{2i}}\Big(f_+(x) - f_-(x)\Big) \quad \Rightarrow \quad \frac{d^{2i}}{dx^{2i}}\Big(f_+(1/2) - f_-(1/2)\Big) = 0.$$

Particularly, $f_+(1/2) - f_-(1/2) = 0$ such that $x = 1/2$ is a stationary point. Furthermore, $(x - 1/2)' = a(x - 1/2) + b(x - 1/2)^3 + ..$ for some real numbers a, b; due to symmetry reasons, the second order term is missing in the Taylor expansion at $x = 1/2$. Thus, we obtain a Pitchfork bifurcation at $a = 0$. Using the computer algebra package maxima [5] we work out the coefficients a and b explicitly,

$$\begin{aligned}\mu^{-1}\frac{d}{dt}x &= -x\,\frac{\vartheta(1-x+n_2)}{(x+n_1)+\vartheta(1-x+n_2)} + (1-x)\,\frac{\vartheta(x+n_1)}{\vartheta(x+n_1)+(1-x+n_2)} \\ &= -2\,\vartheta\,\frac{(2\,n+1)\,\vartheta+(2\,n-1)}{(2\,n+1)\,(\vartheta+1)^2}\left(x-\frac{1}{2}\right) + \frac{32\,\vartheta\,(\vartheta+n-\vartheta^2(n+1))}{(2\,n+1)^3\,(\vartheta+1)^4}\left(x-\frac{1}{2}\right)^3 + \mathcal{O}((x-1/2)^4)\end{aligned}$$

For $\vartheta \in (0,1)$, $n > 0$, the coefficient in front of the third order term always is non-zero, while the coefficient in front of the linear term becomes zero at $\vartheta = \vartheta_p$. Hence, we have a pitchfork bifurcation at that parameter.

□

In Fig. 1 (a), we show that pitchfork bifuration. If the parameters are non-symmetrical ($n_1 \neq n_2$, or $\vartheta_1 \neq \vartheta_2$), the pitchfork bifurcation is replaced by one or two saddle-node bifurcations 1 (b), (c), or even no bifurcation at all 1 (d). The deeper reason for this observation is the instability of the pitchfork bifurcation against any perturbation that breaks the symmetry $x \mapsto 1 - x$. The background is the theory about the unfolding of higher-codimensional bifurcation by generic perturbations [2, 3]. We will not discuss the deeper mathematical background here, but simply investigate the observed pattern in Fig. 1. In panel (a), we have the symmetric case, and find the proper pitchfork bifurcation. Panel (b) shows the result if the number of zealots only differs slightly, where the reinforcement-parameter for both groups are assumed to be identical. We still find a reminiscent of the pitchfork bifurcation: The stable branches in (b) are close to the stable branches in (a), and also the unstable branches correspond to each other. For the limit $n_2 \to n_1$, panel (b) converges to panel (a). However, the branches are not connected any more but dissolve in two unconnected parts, and the pitchfork bifurcation is replaced by a saddle-node bifurcation.
In panel (c) and (d), the upper branch visible in panel (b) did vanish, and only the lower branch is present. As ϑ_2 is kept constant ($\vartheta_2 = 0.5$ in panel (c) and $\vartheta_2 = 0$ in panel (d)) and only ϑ_1 does vary, there is no continuous transition to panel (a).

The effect of reinforcement for a given group is similar to an increase of the number of that group's zealots. If the reinforcement of one group is distinctively stronger than that of the other group, persons recruited by this group will – due to the reinfrocement – stay (long) within this group. The group will dominate the population. In panel (d), the second group has only 1/10 of the zealots of the first group, but is able to take over if the members of that group do an extreme reinforcement ($\vartheta_1 \ll 1$). However, if both groups reinforce themselves, the mechanism is kind of symmetrical, with a bistable setting as the consequence.

A.5 Vaccination data analysis

The data used are made available by the Robert-Koch-Institute, and have been published in [1, 6, 4]. The web pages for the measles data are located in the URL's ("Tabellen")
https://www.versorgungsatlas.de/themen/versorgungsprozesse?tab=3&uid=76&cHash=15379e83482f9325cf011f690c059c26 (accessed 2'nd Mai 2021)
https://www.versorgungsatlas.de/themen/versorgungsprozesse?tab=3&uid=43&cHash=31605ab96524f1a101ec8e3aac07e388 (accessed 2'nd Mai 2021)
and that for meningoccoci https://www.versorgungsatlas.de/themen/versorgungsprozesse?tab=4&uid=75&cHash=08f43064449be9c3947a6ffd61e0e09a (accessed 2'nd Mai 2021)

The GIS-data used are available at the URL
https://gdzshopv-lpz.bkg.bund.de/index.php/default/catalog/product/view/id/773/s/nuts-gebiete-1-250-000-stand-01-01-nuts250-01-01/category/8/?___store=default

The R-code used to analyze the data is available at the GitHub repository https://github.com/jomuemathe/EchoChambersVaccinationHesitancy.

We fit each year separately, assuming that we sample from a quasi-equilibrium, where the parameters change so slowly that the distribution is well approximated by an equilibrium distribution.

To create the graph, indicating which districts are neighbors, we simply identified districts with common boundaries in GIS data, and defined them as neighbors (see Fig. 2).

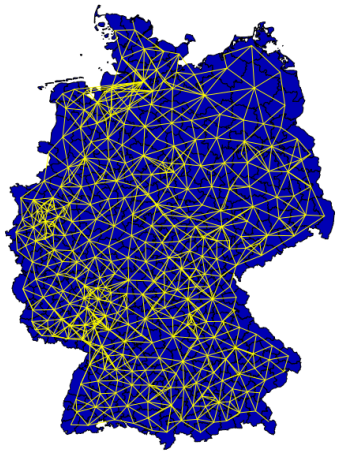

Figure 2: Neighbor-graph as defined for the districts in Germany. Black lines: boundaries of districts; yellow lines: edges between districts (districts are represented by their center of gravity).

Measles We present here all results for the measles vaccination data.

Decoupled model

year	N_1	N_2	θ_1	θ_2	LL tst	KS(reinf)	KS (zealot)	mean
2008	59.64	15.50	250.71	92.65	6.88e-07	0.072	0.0011	0.86
2009	57.47	22.38	213.05	102.61	4.84e-08	0.24	0.0038	0.78
2010	53.14	17.97	188.38	82.01	4.11e-06	0.40	0.019	0.80
2011	47.32	18.49	177.11	91.58	2.30e-07	0.23	0.0018	0.80
2012	50.91	18.56	189.53	92.49	2.07e-06	0.57	0.014	0.81

Spatial model

year	N_1	N_2	θ_1	θ_2	γ
2008	45.29	11.90	317.61	90.70	1024.70
2009	49.49	19.86	271.88	116.27	540.52
2010	41.33	14.35	237.79	88.04	593.66
2011	47.14	15.72	259.09	93.55	556.15
2012	38.42	14.15	243.34	93.59	700.49

If we exclude Saxonia (as it has for meningococci slightly different rules for vaccination), we obtain

year	N_1	N_2	ϑ_1	ϑ_2	γ
2008	46.72	12.46	328.42	95.90	1019.21
2009	53.81	21.56	294.87	126.26	522.32
2010	44.01	15.26	250.89	93.33	574.34
2011	48.73	16.43	269.03	98.30	549.74
2012	40.73	15.20	258.63	100.94	690.08

The parameters are slightly different if we exclude Saxonia, but thee is no fundamental difference to the analysis of all data.

Meningocci Infection We present here all results of the Meningocci vaccination.

Decoupled model

year	N_1	N_2	ϑ_1	ϑ_2	LL tst	KS(reinf)	KS (zealot)	mean
2009	22.11	13.76	84.82	70.80	8.66e-12	0.75	0.0013	0.76
2010	28.68	13.45	108.34	68.03	1.25e-10	0.57	0.0028	0.78
2011	29.19	13.89	119.42	75.99	2.62e-14	0.46	0.00069	0.79
2012	41.39	13.93	159.23	67.96	2.56e-12	0.57	0.0013	0.80
2013	39.58	14.79	157.14	75.99	2.14e-13	0.56	0.00090	0.80

Spatial model

As Saxonia has slightly different recommendations with respect to the meningococci vaccination, these data are left out (and are missing in the original data set).

year	N_1	N_2	θ_1	θ_2	γ
2009	16.83	10.56	91.10	62.012	248.97
2010	22.39	10.66	116.66	62.77	255.67
2011	26.19	11.87	144.67	73.77	277.62
2012	48.82	12.55	223.89	63.24	286.69
2013	39.54	12.52	192.78	69.66	273.14

That is, the parameters for the spatial model are slightly different, but there is no fundamental difference to the analysis of all data.

Elasticities The table with the elasticities show a common pattern for both diseases and all years.

name	year	Elast(N_1)	Elast(N_2)	Elast(ϑ_1)	Elast(ϑ_2)
Measles	2008	0.21	-0.28	-0.133	0.22
Measles	2009	0.48	-0.58	-0.34	0.46
Measles	2010	0.38	-0.45	-0.24	0.33
Measles	2011	0.35	-0.47	-0.24	0.38
Measles	2012	0.32	-0.42	-0.21	0.34
Meningo	2009	0.41	-0.64	-0.32	0.60
Meningo	2010	0.42	-0.56	-0.32	0.50
Meningo	2011	0.41	-0.56	-0.33	0.53
Meningo	2012	0.54	-0.55	-0.40	0.46
Meningo	2013	0.49	-0.56	-0.38	0.48

B SI Figures

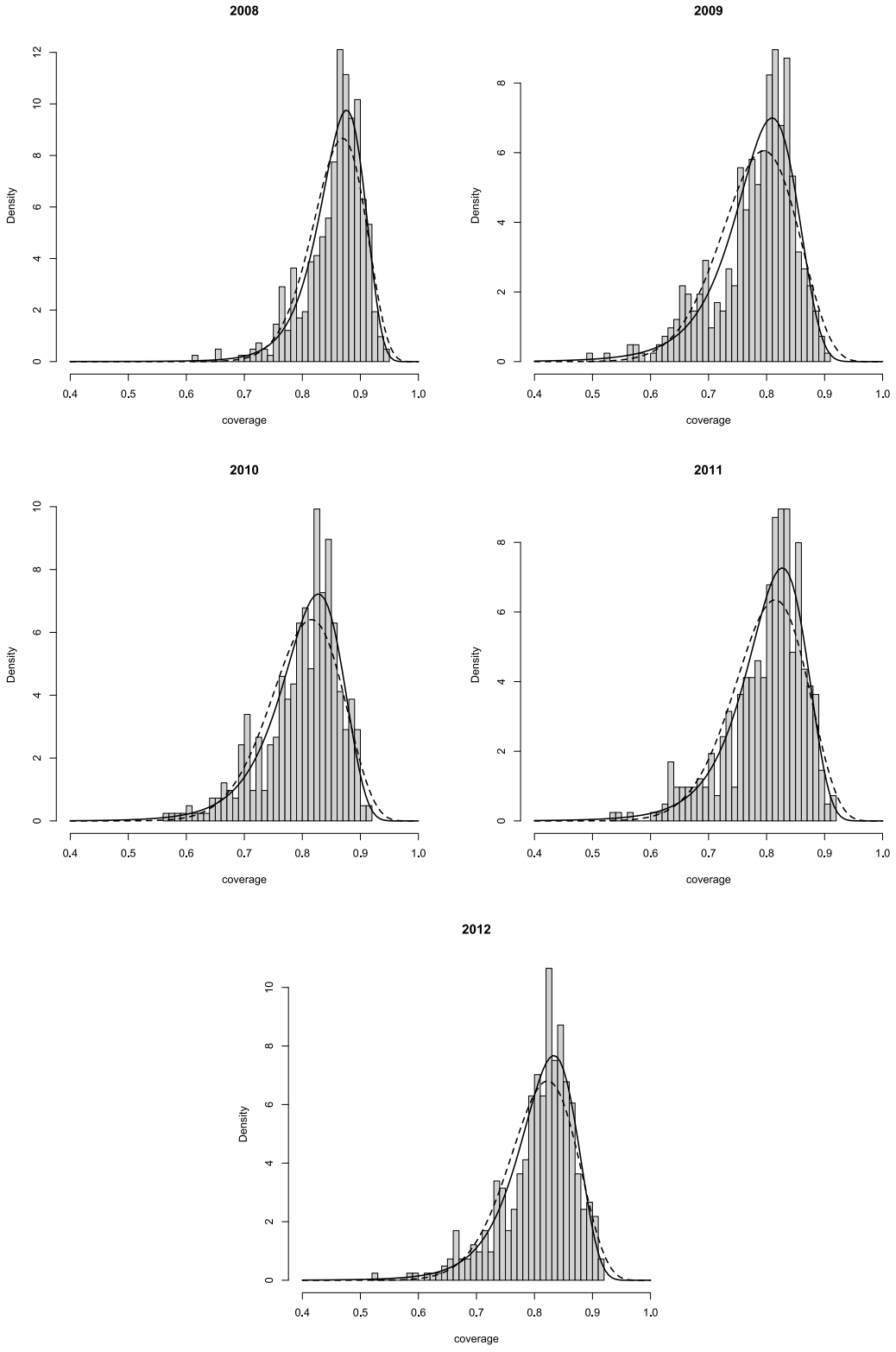

Figure 3: Histograms for the measles vaccination coverage (decoupled model). Solid line: Probability density with reinforcement, dashed line: probability density without reinforcement.

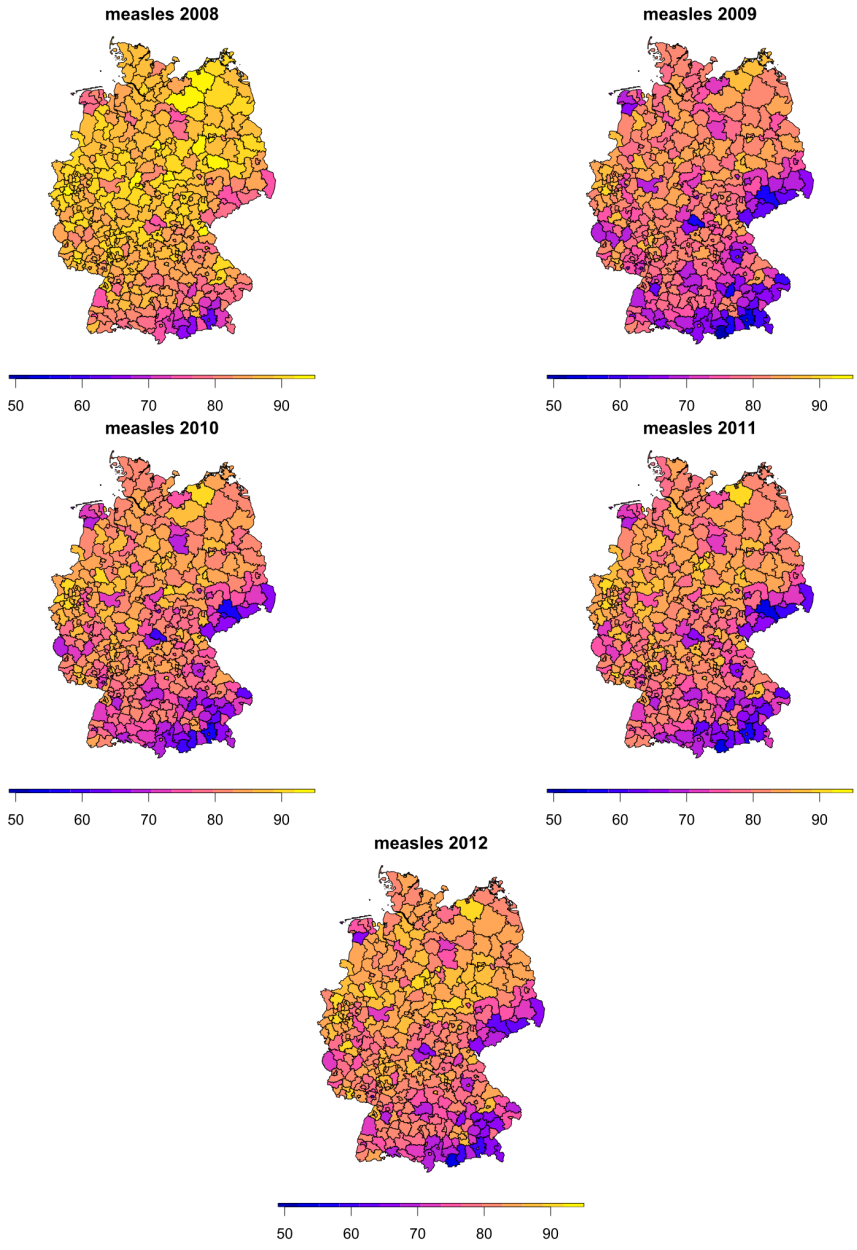

Figure 4: Vaccination coverage (in percent) for measles in Germany.

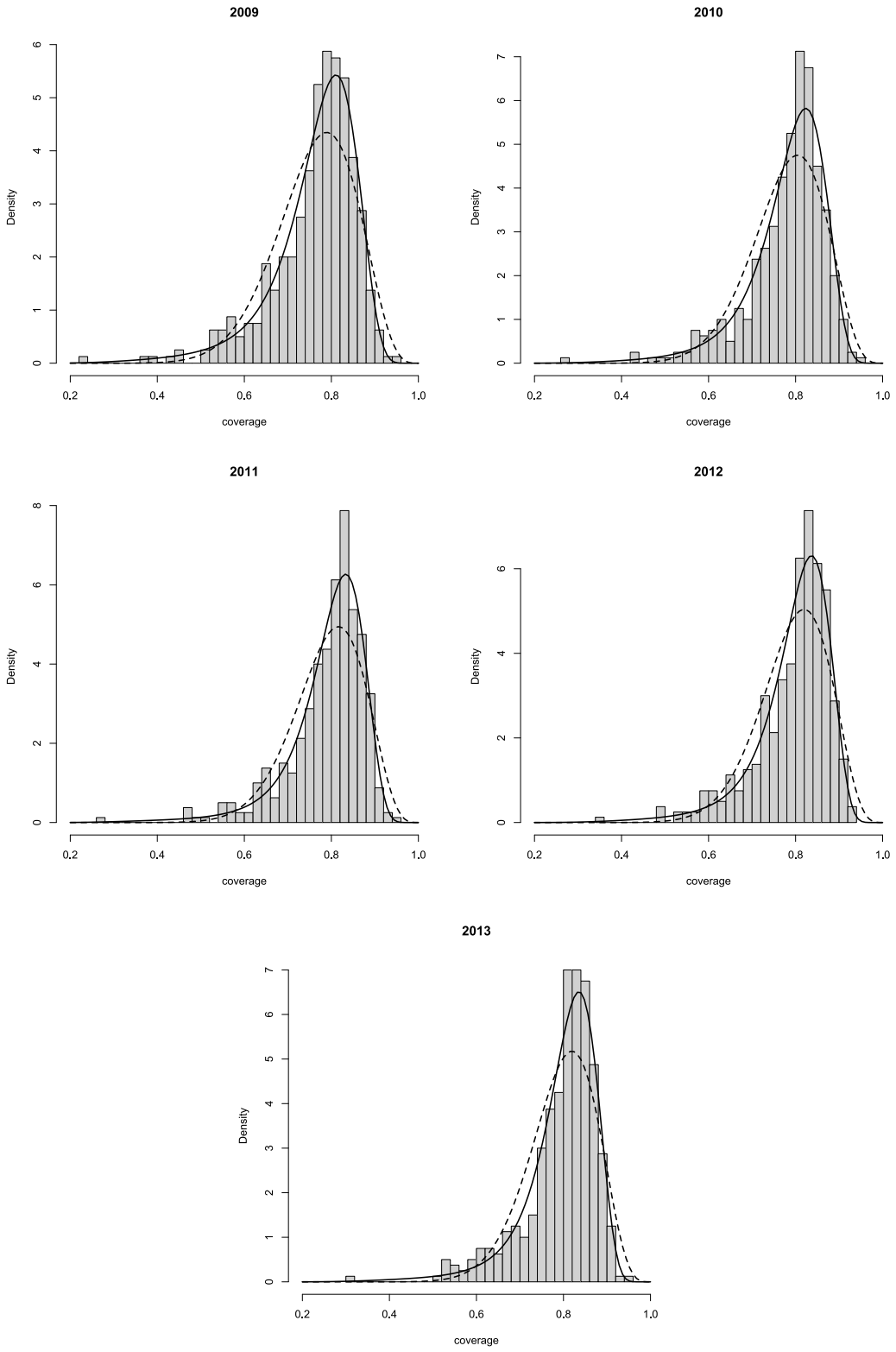

Figure 5: Histograms for the meningicocci vaccination coverage (homogeneous model). Solid line: Probability density with reinforcement, dashed line: probability density without reinforcement.

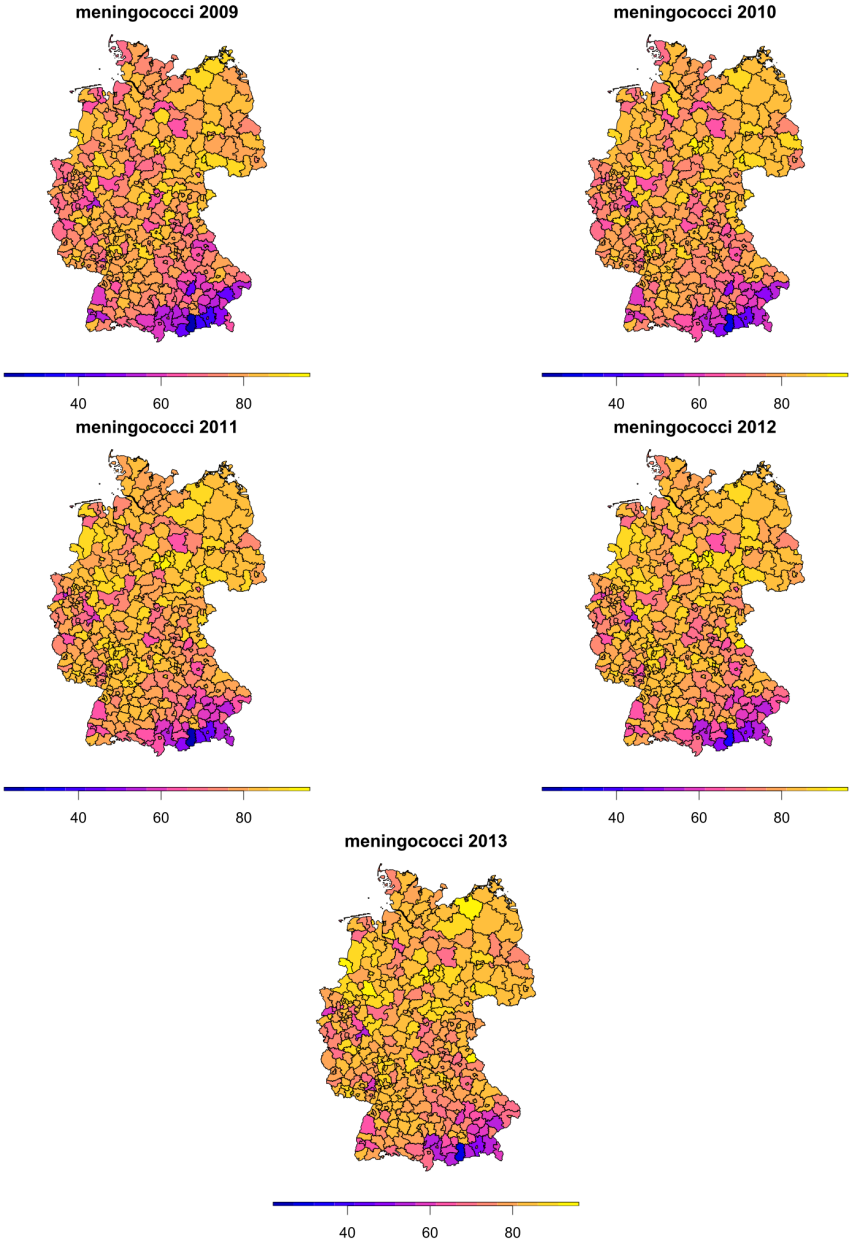

Figure 6: Vaccination coverage (in percent) for meningococci in Germany. Note that the region of Saxonia is missing as its official recommendations for the meningococci vaccination differ from the rest of Germany.

References

[1] B. Goffrier, M. Schulz, and J. Bätzing-Feigenbaum. Masernimpfungen gemäß STIKO-Empfehlungen anhand vertragsärztlicher Abrechnungsdaten von 2009 bis 2014, 2016.

[2] M. Golubitsky and D. G. Schaeffer. *Singularities and Groups in Bifurcation Theory I*. Springer New York, 2013.

[3] M. Golubitsky, D. G. Schaeffer, and I. Stewart. *Singularities and Groups in Bifurcation Theory II*. Springer New York, 2000.

[4] M. L. Greiner, B. Goffrier, M. Schulz, M. Schulz, and J. Bätzing-Feigenbaum. Grundimmunisierung gegen Meningokokken C - Impfraten für die U6-Teilnahmekohorten 2009 bis 2013 im Zeitverlauf, 2016.

[5] Maxima. Maxima, a computer algebra system. version 5.34.1, 2014.

[6] M. Schulz and S. Mangiapane. Masernimpfungen bei Kindern bis zu einem Alter von zwei Jahren, 2013.